6. MINERALOGY AND PETROGRAPHY OF LEG 46 BASALTS

C. Mevel, Laboratoire de Pétrographie, Université Paris VI, Paris, France
and
D. Ohnenstetter and M. Ohnenstetter, Laboratoire de Pétrographie, Université de Nancy I, c/o 140 54037 Nancy Cedex

INTRODUCTION

Leg 46 basalts were recovered at Hole 396B, approximately 160 km east of the Mid-Atlantic Ridge. Basalts 13 million years old, overlain by 150 meters of sediment, have been divided on board ship into eight lithological units, subsequent to petrographic, magnetic, and chemical studies. The upper lithological unit (165 m) is composed of pillows, except for Unit 3, which is a large cooling unit. The lower part is built up of pillow breccias and hyaloclastites. The freshest basalts, slightly vesicular, more often with plagioclase and olivine phenocrysts, were sampled from Units 1 to 4 for chemical and mineralogical studies: 32 basalts were examined in thin section and their bulk chemistry was determined. Electron microprobe analyses were performed on pyroxene, plagioclase, olivine, and titanomagnetite from 12 representative samples.

PETROGRAPHY

Texture, secondary products, and the size variation of the magmatic minerals are shown in Table 1. Thin sections of the basaltic rocks show varying degrees of alteration. The groundmass is always transformed, in varying degree, into smectites. Vesicles are filled with smectites and locally with calcite. Some cross-cutting veins show a similar mineralogy, although zeolites may occur. The two more abundant magmatic minerals, plagioclase and clinopyroxene, are always well preserved. Calcite occurs in cracks in some plagioclase phenocrysts. Olivine is locally transformed into smectites and/or calcite.

Units 1 and 2, separated by interbedded carbonate sediments, consist of fine-grained basalts with sparse olivine and plagioclase microphenocrysts which represent less than 1 per cent of the rocks. Glomerocrysts of these minerals sometimes occur. Plagioclase, olivine, and clinopyroxene are scattered in an abundant groundmass (nearly 30%). In the pillow, rim textures vary from glassy through spherulitic to variolitic, as in Sample 7-2, 42-45 cm. Varioles, small (0.2 mm diameter) in the outer zone, increase in size until (at 0.4 mm diameter) they become coalescent. In the pillow core, hyalopilitic and hyalo-ophitic textures are the more developed.

Unit 3 is a cooling unit. Macroscopically it is composed of dark gray, medium-grained phyric basalts with sparse olivine and plagioclase phenocrysts; texture is intersertal. The two borders are fine grained.

Lithologic Unit 4, more altered than the units above, is built up of a porphyritic pillow sequence. These basalts are gray and fine grained with 15 to 20 per cent phenocrysts. Plagioclase phenocrysts are five times more abundant than olivine phenocrysts. Plagioclase and olivine glomeroporphyritic clots are locally present. Brown chrome spinel occurs as inclusions in plagioclase and as isolated phenocrysts in the groundmass. Plagioclase microlites with pronounced skeletal shape are locally oriented in the abundant mesostatis.

We have examined one sample from lowermost Unit 5. It is grayish brown fine-grained basalt with many patches and veins of calcite and zeolites. The texture is hyalopilitic and trachytic.

CHEMISTRY

Analytical Method

Major elements of 32 basalts have been determined by P. Cambon at the COB using an X-ray fluorescence method similar to that used for shipboard analyses (Bougault and Cambon, 1973; Bougault, in press). Glass and varioles (39 analyses) from Sample 7-2, 73-75 cm, were analyzed using the microprobe. The analytical method is similar to that employed for mineralogical determination (see below). The results are given in Table 2, where chemical and lithologic units are also specified. The bulk chemistry is characteristic of abyssal tholeiites. MgO and SiO_2 are nearly constant, and K_2O is always low in every unit.

Units 2 and 3 (A_3) contain more Ti, Fe, P, and Mn than Unit 1 (A_1-A_2). In Unit 1, the upper part (A_1) is poorer in Ti than the lower A_2. The basalts of Unit 4 (B) are high-alumina tholeiites if the 16.4 per cent Al_2O_3 limit is used (Miyashiro et al., 1969). The Al_2O_3 and CaO enrichment, coupled with low FeO, TiO_2, P_2O_5, and MnO contents when compared with Unit A, may be correlated at first with the abundance of the plagioclase phenocrysts. The fundamental differences in Al_2O_3 and TiO_2 contents between Units A and B and their sub-units may be easily checked in the Al_2O_3-TiO_2 diagram (Figure 1).

The correlation between vertical position and differentiation is inverse in Units A and B. Unit A shows an apparent TiO_2 increase coupled with a slight Al_2O_3 decrease towards the base of the unit: a differentiation inverse to the eruption sequence. In contrast, a normal differentiation pattern occurs in Unit B, in which TiO_2 increases and Al_2O_3 decreases towards the top of the volcanic pile. In each A sub-unit the differentiation trend is similar: TiO_2 increases toward the top of each A sub-unit, especially in A_2, thus indicating a normal differentiation trend with depth. The apparent reversal evolution of Unit A may be a consequence of fractional crystallization of slightly different magma batches. In Unit B, by contrast, as Al_2O_3 decreases and TiO_2

TABLE 1
Summary of Petrographic Features of Basalts From Hole 396B

Lithologic Unit Samples (Interval in cm)	Texture	Plagioclases Phenocrysts	Plagioclases Microphenocrysts	Plagioclases Microlites	Olivine Phenocrysts	Olivine Microphenocrysts	Olivine Microlites	Clinopyroxenes	Opaques	Glassy Groundmass More or Less Altered	Alteration Products	Vesicle Diameter
Unit 1												
5-2, 134-136, #15	Intersertal to hyalo-ophitic		Glomerocrysts 0.8/0.4 mm	0.2/0.03 mm A		Some euhedral crystals, sometimes rounded, 0.6 mm A	0.04 mm	0.05 mm A	Granules	+	Calcite smectite	+
7-1, 106-108, #10	Hyalo-ophitic			0.2/0.05 mm A			0.05 mm anhedral A	Cerviconic and axiolitic A	Granules	+	Calcite	
7-2, 42-45, #5	Glassy-variolitic to spherulitic; varioles size 0.2 to 0.4 mm			0.2/0.3 mm A		0.8/0.2 mm A	+	+	+	+ Varioles A Glass A	Calcite	+
7-2, 73-75, #7B	Intersertal			0.6/0.02 mm		1.6/0.7 mm rounded		+	+	+	Smectite	
8-2, 43-45, #4B	Hyalo-ophitic			0.6/0.4 mm A			0.1 mm A	Axiolitic A	Granules	+	Smectite	+
9-1, 40-49, #60	Hyalo-ophitic		0.6/0.2 mm	0.3/0.02 mm A			0.1 mm A	Dendritic A	Titanomagnetite A	+		0.1 mm
9-3, 14-16, #2A	Intersertal		0.8/0.2 mm A				0.2 mm A	Axiolitic A 0.2/0.01 mm	0.2 mm	+	Smectite calcite	+
10-1, 43-46, #8	Very sparsely phyric, hyalo-ophitic		2.1/0.2 mm				0.03 mm	Axiolitic	Granules	+	Smectite	
10-2, 59-61, #9	Very sparsely phyric, hyalo-ophitic	6/3 mm with melt inclusions		0.7/0.02 mm			0.1 mm	Axiolitic	+	+	Smectite calcite	
11-1, 87-99, #108	Intersertal			0.5/0.02 mm			0.05 mm skeletal	Axiolitic	Granules	+	Smectite calcite	
11-2, 18-20, #2	Very sparsely phyric, intersertal			0.5/0.03 mm A		0.5 mm	0.5 mm	Axiolitic A	Granules	+	Smectite	0.2 mm
12-1, 110-112, #7	Very sparsely phyric, intersertal		0.9/0.6 mm	0.6/0.04 mm			0.2 mm	Axiolitic	Granules	+	Smectite	
Unit 2												
13-2, 137-140, #13	Spherulitic			0.2/0.02 mm bow-ties			0.04 mm skeletal	Dendritic	Granules	+	Smectite calcite in veins	0.2 mm
14-1, 16-21, #3	Very sparsely phyric, spherulitic			0.5/0.03 mm bow-ties		1.2/1.05 mm	0.2/0.04 mm	Axiolitic	Granules	+	Smectite	0.2 mm vesicles and mafic spherules
14-2, 113-115, #11	Intersertal		4.3/0.1 mm A				0.15 mm granular	Axiolitic, fan-shaped; 0.1 mm A	Grains titanomagnetite A	+	Smectite	0.2 mm
14-3, 70-72, #5C	Very sparsely phyric, intersertal		0.9/1.07 mm	0.7/0.05 mm			0.05 mm	Axiolitic	Grains euhedral	+	Smectite	
Unit 3												
15-1, 120-128, #12E	Intersertal			1/0.05 mm			0.05 mm	Axiolitic, fan-shaped	Granules	+	Smectite	
15-2, 79-81, #17	Intergranular		1.6/1 mm	2/0.1 mm			0.5 mm granular A	0.5 mm granular A	Grains 0.03 mm A	+ A	Smectite	0.2 mm
15-2, 99-107, #2A	Intersertal to intergranular		1.2/0.5 mm	1.8/0.1 mm			0.1 mm grains	0.14 mm grains	Grains skeletal 0.14 mm	+	Smectite calcite	0.4 mm
15-4, 114-116, #7	Intersertal		2.5/1.5 mm A	0.8/0.05 mm A			0.14 mm grains skeletal A	0.25 mm grains A	Grains 0.07 mm skeletal	+	Smectite	0.3 mm
15-5, 16-18, #2B	Intersertal		3/1.4 mm	0.2/0.08 mm			Grains 0.07 mm	Grains 0.14 mm skeletal	Grains 0.07 mm	+	Smectite calcite	0.2 mm
Unit 4												
16-1, 28-30, #4	Porphyritic, hyalo-ophitic to intersertal	3/1 mm euhedral melt inclusions		0.5/0.03 mm	2 mm rounded A		0.14 mm	Axiolitic A	Oxides granules Cr-spinel	+	Calcite smectite	0.4 mm
16-3, 34-41, #48	Porphyritic, hyalo-ophitic	5/3 mm melt inclusions		0.4/0.03 mm	2 mm euhedral or rounded		0.15 mm	Axiolitic 0.07 mm	Granules	+	Smectite calcite zeolites	0.4 mm
18-1, 55-57, #4C	Porphyritic, intersertal	3/1 mm melt inclusions		0.6/0.04 mm A	1 mm rounded		0.1 mm A	Axiolitic A	Oxides granules and Cr-spinel 0.07 mm	+	Smectite calcite	0.14 vesicles and spherules 1 mm
20-1, 65-69, #4	Porphyritic, hyalo-ophitic	5/3 mm		0.2/0.02 mm	3 mm rounded		0.16 mm	Axiolitic	Grains 0.04 mm	+	Smectite calcite	0.6 mm vesicles and mafic spherules; 0.4 mm

20-5, 84-93, #9C	Porphyritic, hyalo-ophitic	5/2 mm melt inclusions	0.4/0.03 mm	1.5 mm	0.17 mm rounded	Axiolitic	Oxides granules 0.14 mm and Cr-spinel	+	Calcite smectite zeolites in veins	0.4 mm
21-1, 80-91, #10	Porphyritic, hyalo-ophitic to intersertal	3/1.5 mm glomerophenocrysts	0.4/0.03 mm	1 mm	0.02 mm rounded	Axiolitic	Oxides in grains and skeletal Cr-spinel	+	Smectite calcite	
21-2, 16-24, #2	Porphyritic, hyalo-ophitic	3/1.5 mm melt inclusions	0.04/0.03 mm	1 mm rounded	0.1 mm	Axiolitic	Oxide grains and Cr-spinel	+	Smectite calcite	Vesicles 0.1 mm
22-2, 61-73, #3C	Porphyritic, hyalo-ophitic	2.5/1 mm glomerophenocrysts A	0.4/0.03 mm A	1.5/1 mm calacalstic A	0.2 mm	Axiolitic A	Oxides grains and Cr-spinel	+	Smectite calcite and zeolite in veins	0.4 mm and mafic spherules
22-2, 110-120, #7C	Porphyritic, hyalo-ophitic	3/1 mm melt inclusions A	0.4/0.03 mm A	1 mm rounded A	0.4 mm A	Axiolitic, fan-shaped A	Oxides and Cr-spinel	+	Calcite smectite	Vesicles
22-3, 104-107, #7B	Porphyritic, hyalo-ophitic	3/1.5 mm	0.5/0.03 mm	1 mm	0.2 mm rounded	Axiolitic	Granules	+	Calcite smectite zeolites	
Unit 5										
24-1, 51-53, #9	Pilotaxitic, fluidal		0.4/0.02 mm bow-ties and microlites		0.4 mm skeletal	Dendritic	Granules	+	Calcite zeolites smectite in veins	0.2 mm

increases from B_2 to B_1 — towards the top — B_1 may have been derived from B_2 through a plagioclase fractionation.

Variation diagrams relating FeO/MgO to Fe and Ti oxides show features similar to those noted above (Figure 2). FeO/MgO (1 to 1.5) increases towards the bottom in Unit A and normally towards the top in Unit B. Glass and varioles from Sample 396B-7-2, 42-45 cm are also shown in Figure 2 (by the areas enclosed by solid lines) and reported in Table 3; the details of these areas appear in Figure 3. The FeO/MgO ratios of varioles and glass are lower than that of the host rock but similar to those of the Unit A basalts. MgO depletion in the slightly altered pillow rim would explain in the low FeO/MgO ratio of the host rock (Honnorez and Bohlke, in press). Varioles are richer in TiO_2 than glass and host rock. Fe distribution is similar in varioles and glass; Fe oxide increases with ratio increase. This trend shown by varioles and glass in a single pillow is similar to the normal evolution of abyssal tholeiites. The narrow compositional range between varioles and basalts excludes an immiscibility process for the variole genesis. Undercooling is the more probable explanation of their formation (Lofgren, 1974).

PHASE CHEMISTRY

Electron microprobe analyses were obtained for 12 samples of lithologic Units 1 to 4. The minerals were analyzed using the CAMECA MS 46 microprobe at the University of Paris. The analytical conditions were as follows: accelerating voltage 15 kV, specimen current 30 nA, counting time 50 seconds for olivine and pyroxene and 25 seconds for plagioclase. Natural minerals were used as standards. The microprobe data were reduced on the CIRCE IBM 370 computer employing the EMPEDAR program (Rucklidge and Gasparini, 1969). In Sample 396B-7-2, 42-45 cm, the fine grain size of the pryoxenes does not permit their analyses. This is also true for opaque oxides in many samples.

We analyzed 243 pyroxene samples, using the microprobe. Representative selected samples are reported in Table 4. The pyroxenes, slightly brown in thin section and scattered in the groundmass, constitute one of the last crystallizing phases. The habit is axiolitic, dendritic, and comb-like (except in the cooling unit of Core 15, where it is more often granular). These pyroxenes fall always in the augite-salite field for Units 1, 2, and 4. The pyroxenes of the cooling unit are restricted to the augite field. Al_2O_3 and TiO_2 contents are high and show wide varations throughout the unit. TiO_2 contents of Units 1 and 2 are the highest. In the porphyritic basalt of Unit 4, Al_2O_3 content reaches the highest values (up to 8.69%).

In the Ca-Mg-Fe diagram (Figure 4, pyroxenes of Unit 1 fall in the same field, despite the dispersion. There is no obvious trend, only a slight Fe-Mg variation. Sample 396B-5-2, 134-136 cm exhibits a Mg-Ca variation. In Unit 2, pyroxenes of the analyzed sample fall in the same area, but Mg is nearly constant. In Unit 3, pyroxenes fall in the augite field and are relatively more magnesium-rich than pyroxenes of the unit above. An iron-enrichment trend at nearly constant Mg is evident for the two analyzed samples. Such a trend is usually considered a result of rapid metastable crystallization linked to undercooling (Kirkpatrick, 1976). This trend is curiously well-developed in this cooling unit

TABLE 2
Chemical Analyses of the Basalts From Hole 396B

Sample	5-2 134-136	7-1 #10	7-2 #5	7-2 #7B	8-2 #4B	9-1 #6D	9-3 #2A	10-1 #8	10-2 #9	11-1 #10B	11-2 #2	12-1 #7	13-2 #13	14-1 #3	14-2 #11
Lithological Unit	1	1	1	1	1	1	1	1	1	1	1	1	1	2	2
Chemical Unit	A_1	A_1	A_1	A_1	A_1	A_2	A_2	A_2	A_2	A_2	A_2	A_2	A_2	A_3	A_3
SiO_2	49.46	49.90	48.82	49.41	49.44	48.99	50.22	49.89	49.22	49.19	49.46	50.01	49.23	48.91	49.52
Al_2O_3	15.22	15.72	16.02	15.24	15.15	15.95	15.50	14.91	15.23	15.06	15.03	14.93	15.22	15.21	15.09
$Fe_2O_3^+$	10.37	10.01	10.93	10.14	10.45	11.24	9.92	10.31	10.53	10.74	10.55	10.58	10.72	11.28	11.11
MnO	0.17	0.17	0.18	0.16	0.17	0.18	0.15	0.16	0.17	0.17	0.17	0.16	0.18	0.18	0.17
MgO	8.08	7.77	6.80	8.42	8.03	6.89	7.10	7.60	7.38	7.75	7.50	7.65	7.74	7.80	7.37
CaO	12.00	12.24	12.29	11.80	11.57	12.26	11.93	11.51	11.88	11.59	11.55	11.48	11.65	11.23	11.11
Na_2O															
K_2O	0.28	0.24	0.17	0.23	0.27	0.27	0.23	0.28	0.26	0.24	0.24	0.26	0.15	0.26	0.26
TiO_2	1.42	1.43	1.48	1.41	1.52	1.61	1.59	1.56	1.53	1.54	1.54	1.52	1.55	1.67	1.65
P_2O_5	0.15	0.13	0.16	0.13	0.14	0.18	0.15	0.15	0.15	0.14	0.15	0.13	0.15	0.18	0.17
L.O.I. 110°	0.70	0.29	0.87	0.65	1.42	0.93	0.50	1.36	0.59	0.64	0.41	1.21	0.40	0.66	0.35
L.O.I. 1050°	0.38	0.59	0.66	0.46	1.24	0.70	0.64	0.88	0.67	0.38	0.45	1.01	0.38	0.65	0.68

composed of the largest minerals. Nevertheless, the presence of altered glass testifies to the efficiency of rapid cooling. This trend is also recognizable in Unit 4 pyroxenes, which are slightly richer in Ca and Mg.

Plagioclases

Selected plagioclase analyses, reported in Table 5, have no K-feldspar component. Plagioclase microlites show a narrow compositional range of An_{63-73}. The highest An values occur in Unit 2. In Unit 3 two generations of feldspar may be present. The big ones are calcic (An_{65-71}) than the small ones (An_{47-51}). The plagioclase phenocryst of Unit 4 has a nearly constant composition in the core (An_{75-85}; $_{75-89}$); the narrow rim is more sodic (An_{64-68}; $_{70-75}$) and shows values similar to those of the coexisting microlites (An_{65-73}).

Olivines

Selected olivines are reported in Table 6. Olivine is magnesian in all the units (Fo_{78-88}). Unit 4 exhibits the more magnesian olivine (Fo_{83-88}). Olivine phenocrysts do not appear to be significantly zoned, and have the same composition as the olivine microlites.

Opaque Oxides

Titanomagnetites were analyzed in Samples 396B-9-1, 40-49 cm and 396B-14-2, 113-115 cm. Partial analyses are summarized in Table 7. The FeO-TiO_2 contents are similar to those reported by Mazzullo et al. (1976).

CONCLUSION

1. Bulk chemistry and chemical data are consistent with the lithologic and chemical unit defined aboard ship. Basalts are typically abyssal tholeiites; the Unit 4 porphyritic basalts are high-alumina tholeiites.

2. Unit A is more fractionated than Unit B. Unit A shows an apparent inverse evolution with depth, whereas in Unit B the upper basalt may have evolved from the lower basalt through a plagioclase fractionation.

3. Varioles have a compositional range similar to that of the basalt, and were formed by an undercooling process.

4. Augite and salite from Units 3 and 4 show a Fe-Ca variation at nearly constant Mg, a feature characteristic of metastable crystallization which occurs during undercooling.

REFERENCES

Bougault, H., in press. Major elements: analytical chemistry on board and preliminary results.

Bougault, H. and Cambon, P., 1973. Dispersive X-ray fluorescence analysis on board oceanographic vessels. *Marine Geology*, v. 15, p. 37-41.

Honnorez, J. and Bohlke, J.K., in press. Oxidation front during the low-temperature submarine alteration of Mid-Atlantic Ridge basalts, *EOS*.

Kirkpatrick, R.J., 1976. Towards a kinetic model for the crystallization of magma bodies, *J. Geophys. Res.*, v. 81, p. 25-65.

Lofgren, G., 1974. An experimental study of plagioclase crystal morphology: isothermal crystallization, *Am. J. Sci.*, v. 274, p. 243-273.

Mazzullo, L.J., Bence, A.E., and Papike, J.J., 1976. Petrography and phase chemistry of basalts from DSDP Leg 34. *In* Yeats, R.S., Hart, S.R., et al., *Initial Reports of the Deep Sea Drilling Project*, v. 34: Washington (U.S. Government Printing Office), p. 245-261.

Miyashiro, A., Shido, F., and Ewing, M., 1969. Diversity and origin of abyssal tholeiite from the Mid-Atlantic Ridge, near 24° and 3°N latitude, *Contr. Mineral. Petrol.*, v. 23, p. 38-52.

Rucklidge, J. and Gasparini, E.L., 1969. Electron microprobe analytical reduction EMPEDAR VII, University of Toronto, Department of Geology.

TABLE 2 – *Continued*

14-3 #5C	15-1 #12E	15-2 #1J	15-2 #2A	15-4 #7	15-5 #2B	16-1 #4	16-3 #4B	18-1 #4C	20-1 #4	20-5 #9C	21-1 #10	21-2 #2	22-2 #3C	22-1 #7C	22-3 #7B	24-1 #9
2	4	4	4	4	4	4	4	4	4	4	4	4	4	4	4	5
A_3	A_3	A_3	A_3	A_3	A_3	B_1	B_1	B_1	B_1	B_2	B_2	B_2	B_2	B_2	B_2	C
50.19	48.86	49.25	49.71	49.78	49.59	49.47	48.97	49.29	48.82	48.62	48.78	49.14	48.36	49.17	49.42	49.10
15.30	15.37	14.91	15.05	15.12	15.03	17.21	17.15	17.07	16.99	17.74	17.57	17.44	18.33	17.91	17.37	16.28
10.68	11.25	11.04	11.05	10.86	10.93	9.19	9.46	9.35	9.25	8.57	8.72	8.65	8.80	8.54	8.61	10.59
0.16	0.19	0.17	0.16	0.17	0.18	0.15	0.15	0.15	0.15	0.14	0.14	0.13	0.15	0.14	0.14	0.17
7.04	7.10	7.96	7.78	7.87	7.28	6.22	7.12	6.90	7.98	7.89	7.42	7.49	7.89	7.20	7.93	7.29
11.33	11.68	11.08	11.10	11.08	11.19	12.72	12.48	12.53	12.44	12.62	12.74	12.54	12.14	12.44	12.51	11.83
0.27	0.28	0.09	0.17	0.18	0.32	0.17	0.20	0.21	0.22	0.14	0.20	0.17	0.28	0.10	0.12	0.26
1.70	1.68	1.66	1.65	1.65	1.67	1.24	1.22	1.23	1.18	1.02	1.04	1.01	0.99	0.99	1.02	1.57
0.17	0.17	0.16	0.16	0.16	0.16	0.13	0.13	0.12	0.12	0.10	0.10	0.11	0.12	0.11	0.10	0.18
1.63	1.00	0.33	0.90	0.87	1.20	1.21	1.54	0.99	0.77	0.90	0.70	0.78	1.25	0.72	0.63	0.66
1.17	1.47	0.04	0.99	0.60	0.82	1.15	1.20	0.88	0.50	1.09	1.12	1.11	2.75	1.21	0.80	0.56

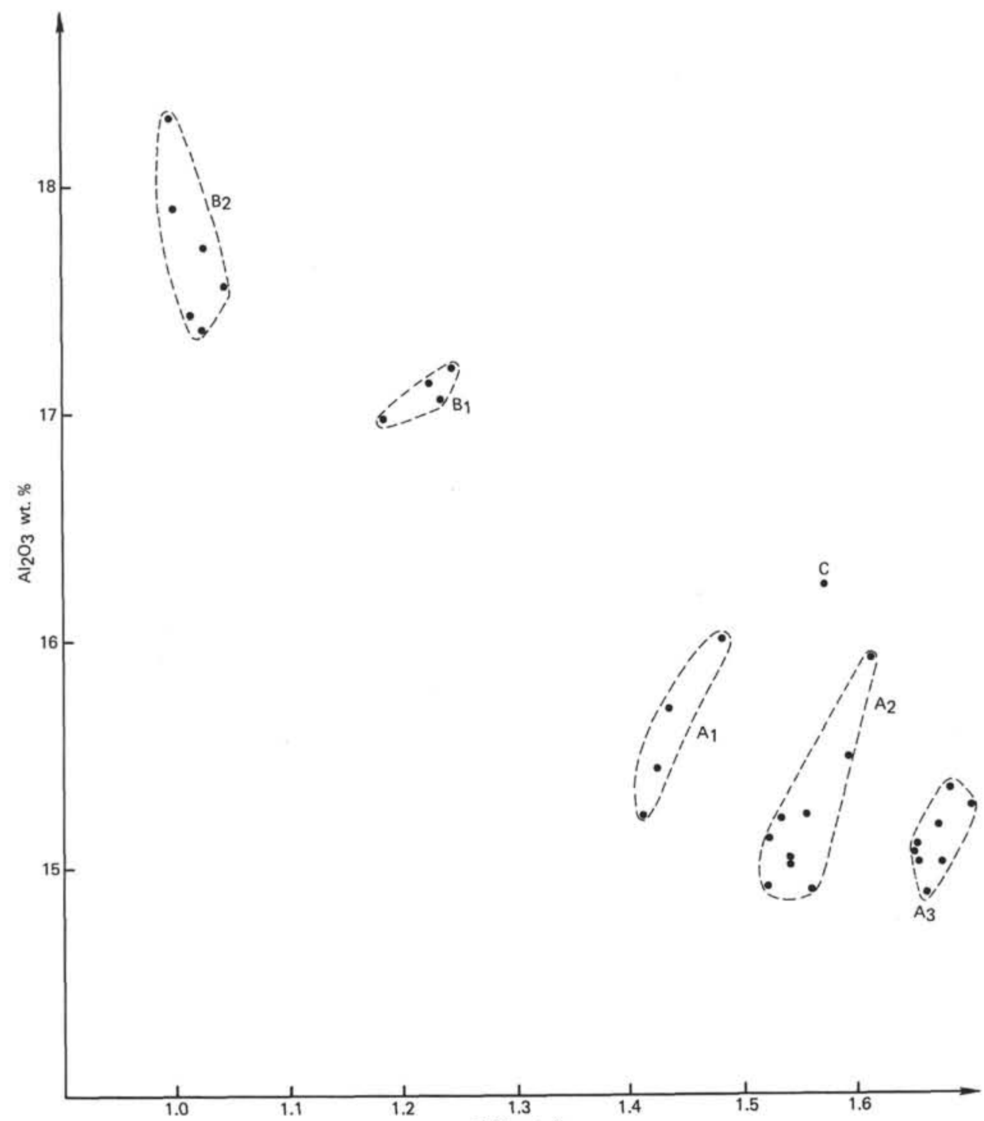

Figure 1. *Al_2O_3 - TiO_2 diagram.*

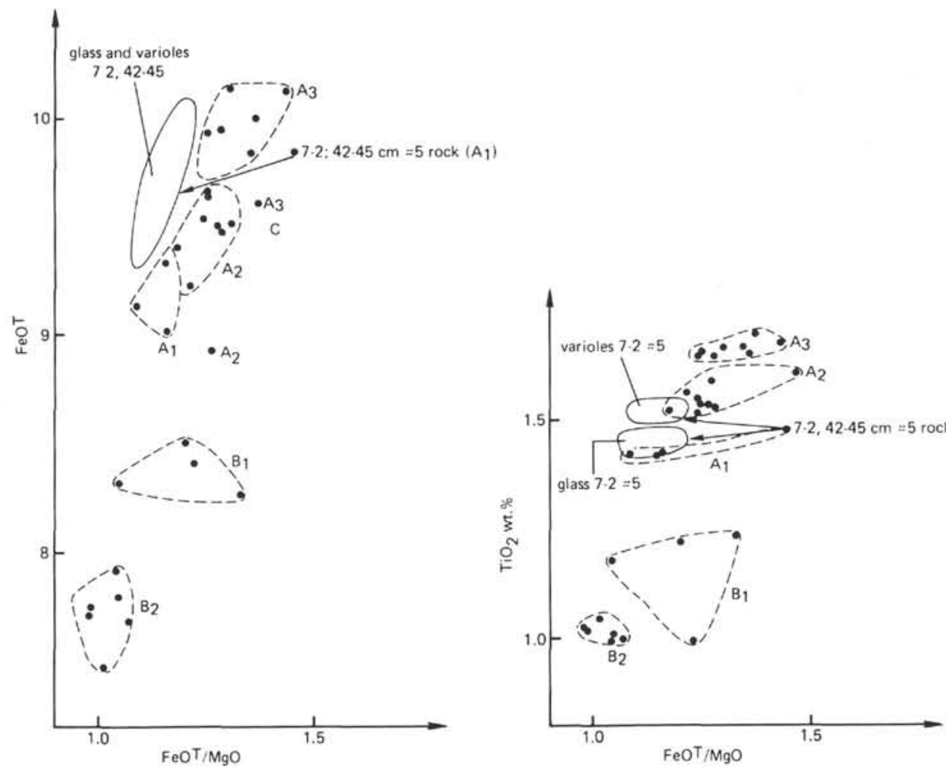

Figure 2. *FeO^T and TiO_2 versus FeO^T/MgO.*

TABLE 3
Chemical Composition of Glass and Varioles of Basalt Sample 396B-7-2, 42-45 cm; Analyzed by Microprobe

						Varioles	
Sample	Glasses			Varioles		Rim	Core
SiO_2	49.99	49.70	50.59	49.08	49.91	49.41	48.68
Al_2O_3	16.72	17.18	16.01	16.82	17.58	16.20	16.10
$Fe_2O_3^+$	9.55	9.48	9.65	10.22	10.98	10.12	9.72
MnO	0.23	0.22	0.23	0.26	0.26	0.52	0.23
MgO	8.84	8.76	8.72	9.01	6.08	8.60	8.28
CaO	11.24	11.34	11.83	11.11	11.58	11.44	12.05
Na_2O	2.35	2.18	2.16	2.25	2.29	2.59	2.59
K_2O	0.15	0.13	0.10	0.09	0.17	0.14	0.08
TiO_2	1.44	1.48	1.52	1.34	1.57	1.64	1.54
Total	100.52	100.47	100.81	100.18	100.42	100.67	99.27

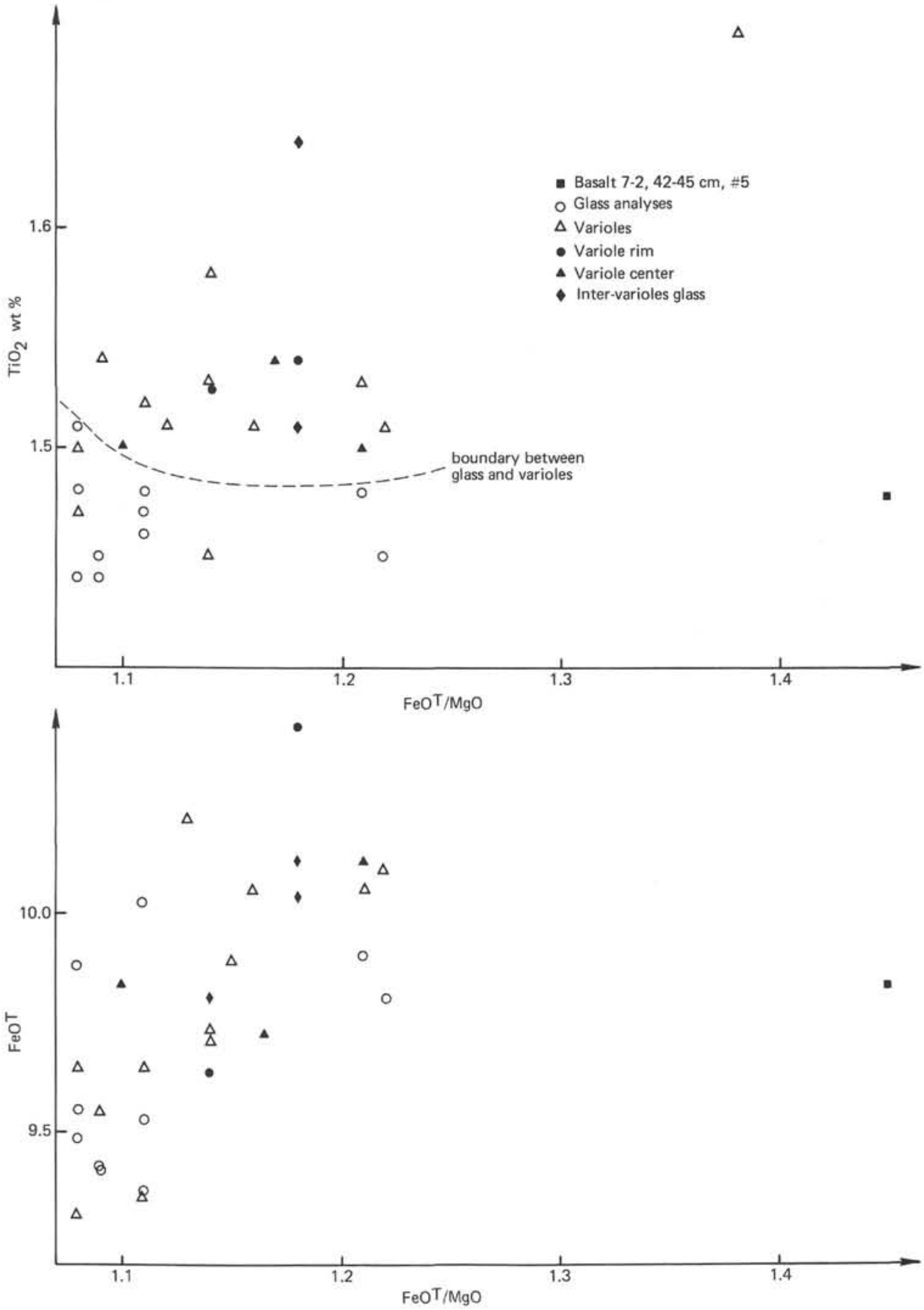

Figure 3. *FeO^T and TiO_2 versus FeO^T/MgO for varioles and glass from Sample 7-2, 42-45 cm basalt.*

TABLE 4
Representative Pyroxenes Analyzed by Microprobe

Sample	5-2, 134-136 cm			7-1, 106-108 cm		8-2, 43-45 cm		11-2, 18-20 cm		14-2, 113-115 cm		
SiO_2	47.87	48.00	48.48	47.01	47.94	44.48	48.41	44.93	45.40	47.22	46.49	44.99
Al_2O_3	5.74	5.21	6.08	5.61	5.38	5.29	3.58	4.78	5.27	5.06	4.61	6.72
FeO^+	11.43	8.46	12.72	12.81	9.32	13.72	12.19	13.52	11.51	12.85	15.57	11.69
MnO	0.30	0.27	0.38	0.32	0.24	0.32	0.35	0.40	0.33	0.33	0.41	0.29
MgO	13.29	15.47	9.76	12.18	13.61	10.17	12.11	11.67	12.01	12.70	12.64	11.76
CaO	19.36	19.49	19.60	19.73	21.41	21.88	19.82	21.54	20.00	19.85	18.62	21.25
Na_2O	0.46	0.36	0.46	0.43	0.49	0.50	0.43	0.61	0.42	0.51	0.46	0.48
TiO_2	2.12	1.70	2.53	1.96	1.66	2.55	2.14	2.26	4.07	2.30	2.36	2.89
Total	100.57	98.95	100.01	100.06	100.05	99.05	99.04	99.70	99.00	100.81	101.16	100.08
Si	1.796	1.807	1.835	1.790	1.802	1.742	1.855	1.746	1.748	1.787	1.773	1.719
Al^{IV}	0.204	0.193	0.165	0.210	0.198	0.244	0.145	0.219	0.239	0.213	0.207	0.281
Al^{VI}	0.005	0.038	0.106	0.042	0.041	–	0.017	–	–	0.013	–	0.022
Ti	0.060	0.048	0.072	0.056	0.047	0.078	0.062	0.066	0.118	0.065	0.068	0.083
Fe	0.359	0.266	0.403	0.408	0.293	0.450	0.391	0.439	0.370	0.407	0.497	0.374
Mn	0.010	0.009	0.012	0.010	0.008	0.012	0.011	0.013	0.011	0.011	0.013	0.010
Mg	0.743	0.868	0.551	0.691	0.763	0.594	0.692	0.676	0.689	0.716	0.719	0.670
Ca	0.778	0.786	0.795	0.805	0.862	0.918	0.814	0.897	0.825	0.805	0.761	0.870
Na	0.034	0.026	0.034	0.032	0.036	0.038	0.032	0.046	0.032	0.038	0.034	0.036
Wo	41.4	40.9	45.5	42.3	44.9	46.8	42.9	44.6	43.8	41.8	38.5	45.5
En	39.5	45.2	31.5	36.3	39.8	30.3	36.5	33.6	36.6	37.1	36.4	35
Fs	19.1	13.9	23	21.4	15.3	22.9	20.6	21.8	19.6	21.1	25.1	19.5

TABLE 4 – *Continued*

15-2, 79-81 cm			15-4, 114-116 cm			16-1, 28-30 cm			18-1, 55-57 cm		22-2, 61-73 cm			22-2, 110-120 cm	
48.84	46.50	47.48	47.43	47.48	46.98	47.92	47.64	48.53	46.12	48.28	47.31	45.63	46.45	46.89	47.69
2.92	6.09	3.79	5.63	3.50	3.70	4.18	5.59	3.25	5.95	3.25	5.55	6.79	7.01	6.89	3.10
14.48	10.08	11.85	9.68	14.09	16.99	9.00	10.73	13.36	10.47	13.65	11.48	9.02	7.83	8.57	14.87
0.47	0.26	0.36	0.30	0.42	0.54	0.31	0.58	0.38	0.27	0.46	0.32	0.24	0.22	0.22	0.35
13.77	12.95	13.74	12.82	12.65	12.14	12.71	13.78	14.30	12.80	14.48	12.40	12.52	12.25	13.40	14.07
17.82	21.29	19.57	20.94	18.50	16.46	21.88	19.62	18.38	21.10	18.08	20.50	22.87	23.28	21.33	18.03
0.43	0.48	0.45	0.53	0.45	0.46	0.66	0.50	0.46	0.30	0.33	0.46	0.48	0.33	0.37	0.33
1.66	2.48	1.95	2.17	1.92	2.19	2.37	2.25	1.44	2.34	1.71	2.08	1.58	2.20	2.07	1.21
100.39	100.12	99.19	99.51	99.02	99.46	100.03	100.69	100.10	99.35	100.23	100.10	99.12	99.41	99.74	99.65
1.856	1.758	1.818	1.796	1.835	1.823	1.804	1.786	1.844	1.760	1.834	1.793	1.744	1.751	1.762	1.834
0.131	0.242	0.171	0.204	0.159	0.169	0.196	0.214	0.146	0.240	0.146	0.207	0.256	0.249	0.238	0.140
–	0.029	–	0.047	–	–	0.034	0.033	–	0.027	–	0.041	0.050	0.064	0.067	–
0.048	0.070	0.056	0.062	0.056	0.064	0.067	0.063	0.041	0.067	0.049	0.059	0.045	0.063	0.058	0.035
0.460	0.319	0.379	0.307	0.455	0.551	0.283	0.336	0.424	0.334	0.434	0.364	0.288	0.248	0.269	0.478
0.015	0.008	0.012	0.010	0.014	0.018	0.010	0.018	0.012	0.009	0.015	0.010	0.008	0.007	0.007	0.011
0.780	0.730	0.784	0.723	0.728	0.702	0.713	0.770	0.810	0.728	0.820	0.700	0.713	0.691	0.751	0.807
0.725	0.862	0.803	0.849	0.766	0.684	0.883	0.788	0.748	0.863	0.736	0.832	0.936	0.944	0.859	0.743
0.032	0.035	0.034	0.039	0.045	0.035	0.048	0.036	0.034	0.022	0.025	0.034	0.035	0.025	0.027	0.025
36.9	45.1	40.8	45.2	39.3	35.3	47	41.6	37.7	44.8	37	43.9	48.3	50.1	45.7	36.6
39.7	38.2	39.9	38.5	37.4	36.2	37.9	40.7	40.9	37.8	41.2	36.9	36.8	36.7	40	39.8
23.4	16.7	19.3	16.3	23.3	28.4	15.1	17.7	21.4	17.4	21.8	19.1	14.9	13.2	14.3	23.6

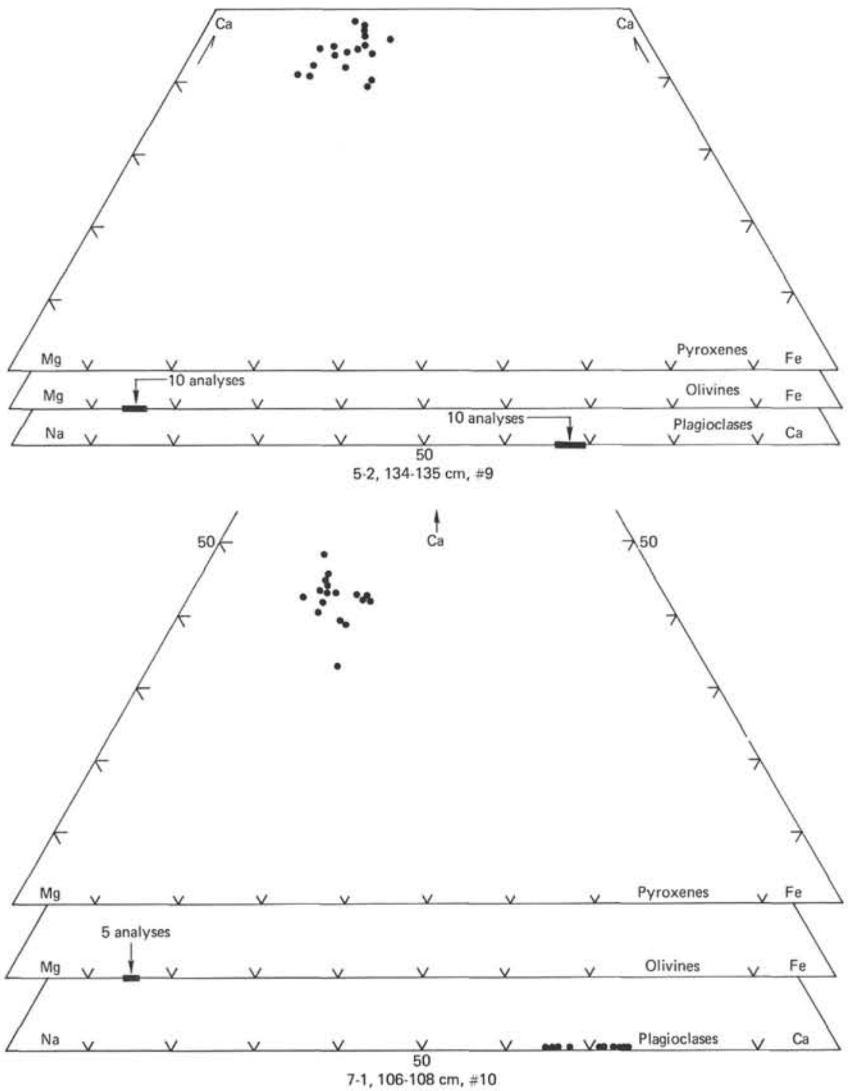

Figure 4. *Ca-Mg-Fe pyroxene compositions, Mg-Fe olivine compositions, and K-Ca-Na plagioclase compositions of the analyzed samples.*

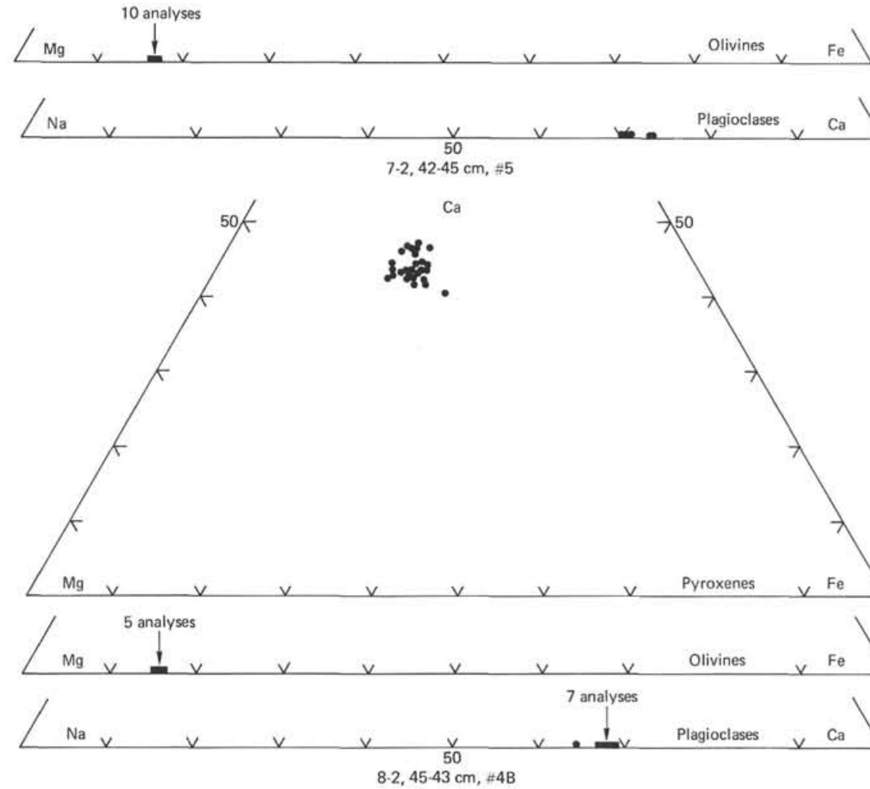

Figure 4. *(Continued).*

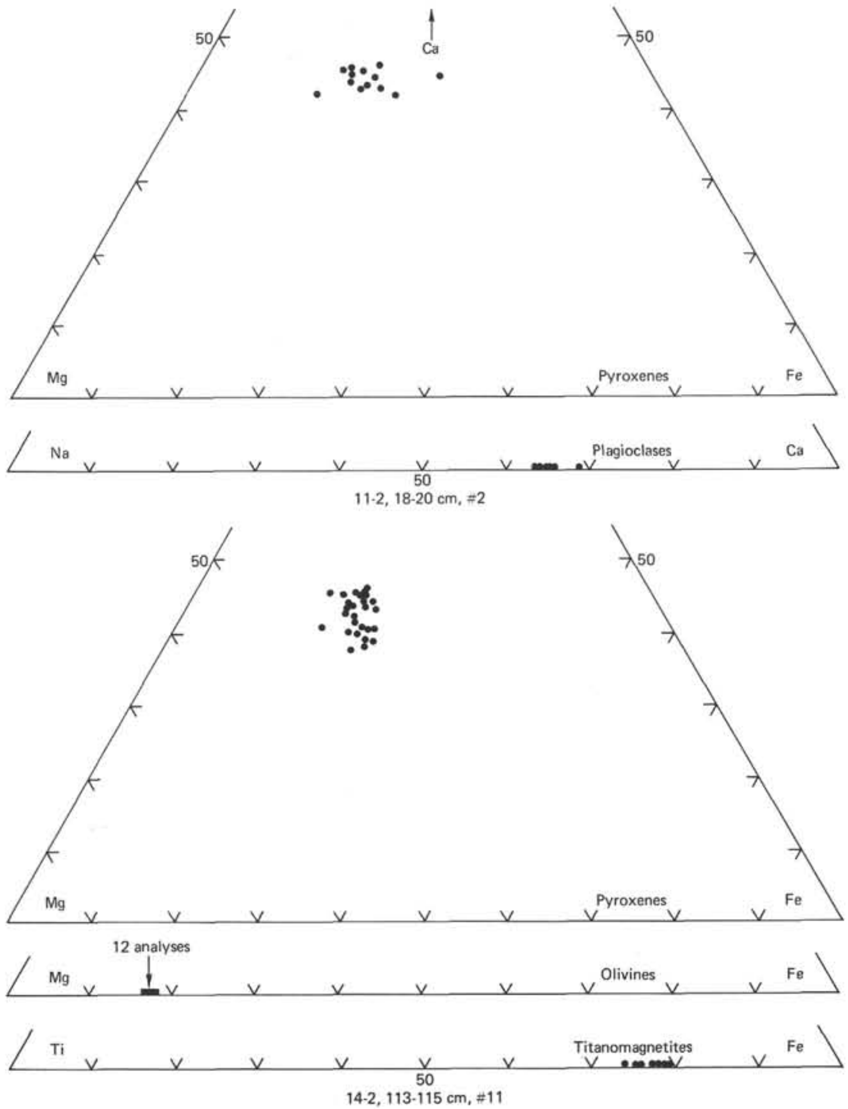

Figure 4. *(Continued).*

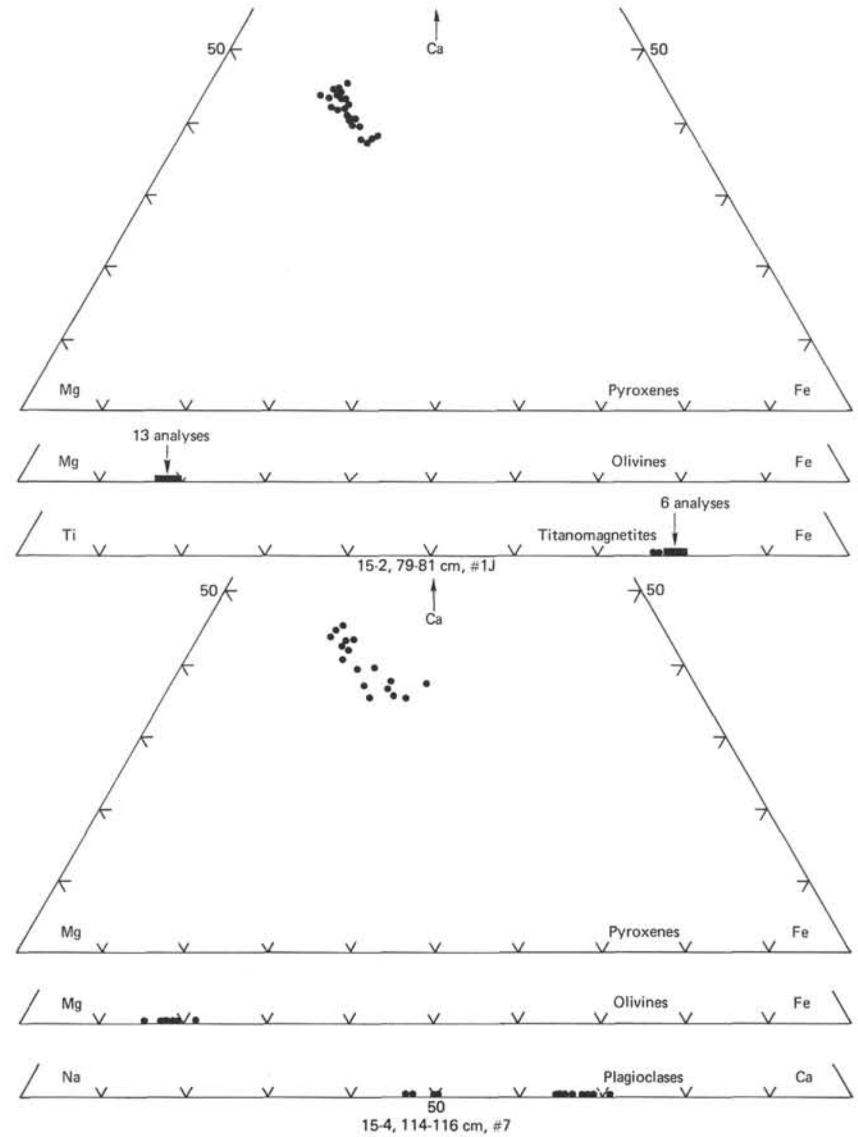

Figure 4. *(Continued).*

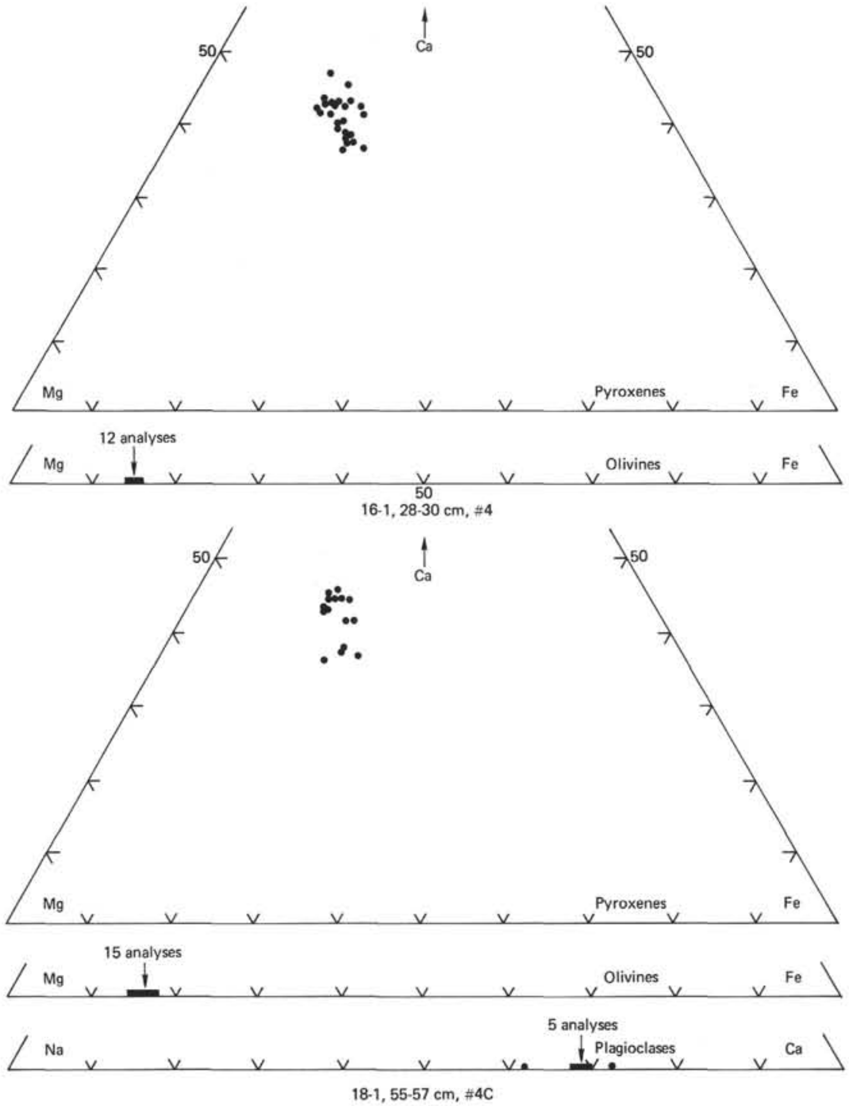

Figure 4. *(Continued).*

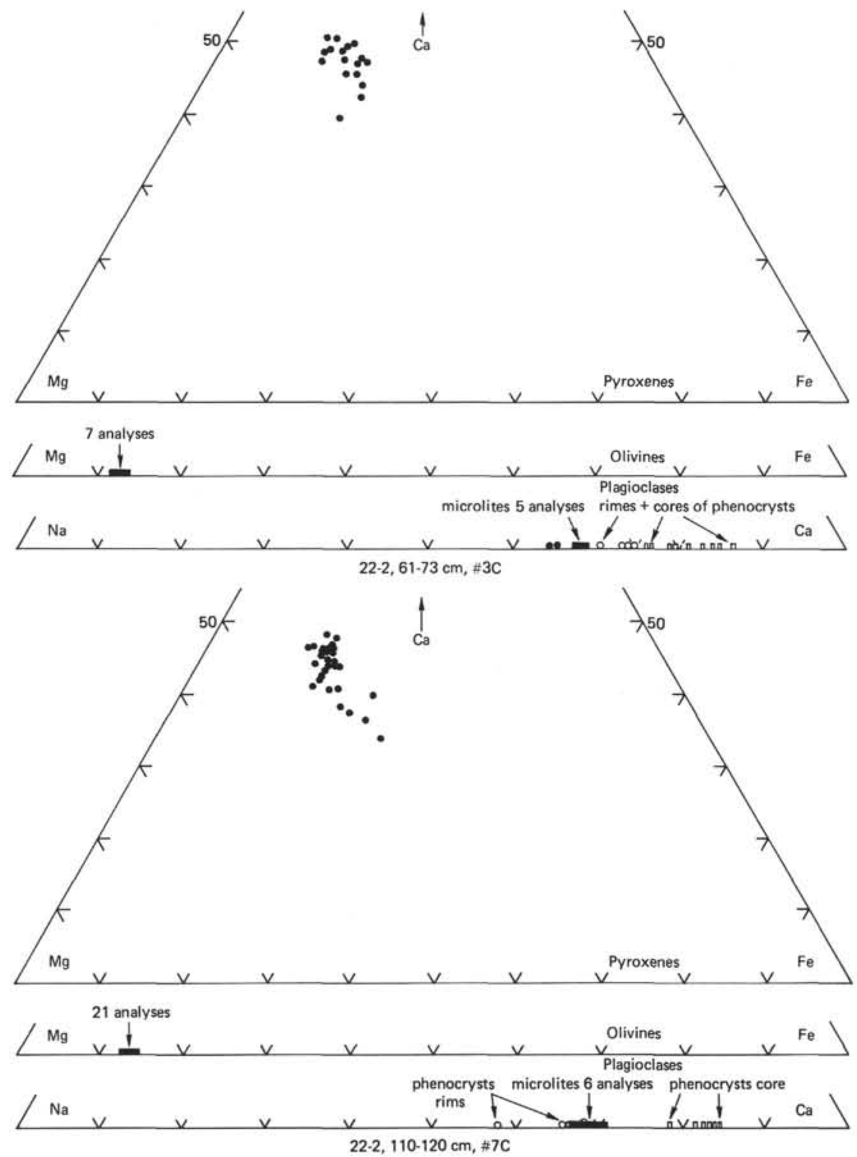

Figure 4. *(Continued).*

TABLE 5
Representative Plagioclase Analyzed by Microprobe

Sample	5-2, 134-136 cm	7-1, 106-108 cm	7-1, 106-108 cm	7-2, 42-45 cm	8-2, 43-45 cm	11-2, 18-20 cm	15-4, 114-116 cm	
SiO_2	52.26	52.71	53.00	51.88	52.03	52.51	52.94	56.50
Al_2O_3	30.42	30.07	30.43	30.75	30.28	29.02	29.99	27.31
CaO	14.42	14.80	13.47	14.26	14.15	13.29	13.77	10.00
Na_2O	3.57	3.05	3.90	3.37	3.63	4.12	3.97	5.59
Total	100.67	100.63	100.80	100.26	100.09	98.94	100.68	99.39
Si	9.437	9.508	9.527	9.398	9.445	9.626	9.543	10.191
Al	6.475	6.394	6.448	6.564	6.840	6.271	6.373	5.806
Ca	2.790	2.861	2.595	2.768	2.753	2.611	2.660	1.932
Na	1.249	1.065	1.360	1.182	1.277	1.463	1.388	1.956
Z	15.92	15.90	15.98	15.97	15.93	15.90	15.92	16
X	4.04	3.93	3.96	3.95	4.03	4.07	4.05	3.89
Ab	30.9	27.1	34.4	29.9	31.7	35.9	34.3	50.3
An	69.1	72.9	65.6	70.1	68.3	64.1	65.7	49.7

TABLE 5 – *Continued*

Sample	18-1, 55-57 cm	22-2, 61-73 cm			22-2, 110-120 cm		
SiO_2	51.84	46.34	48.70	52.19	50.76	47.57	52.09
Al_2O_3	30.87	33.43	31.59	30.45	30.39	33.93	29.84
CaO	14.21	17.26	15.22	14.06	13.98	17.36	14.36
Na_2O	3.55	1.79	2.96	3.68	3.58	2.00	3.38
Total	100.47	98.82	98.47	100.37	98.71	100.86	99.67
Si	9.376	8.621	9.038	9.444	9.352	8.666	9.492
Al	6.581	7.330	6.910	6.494	6.598	7.285	6.410
Ca	2.754	3.440	3.027	2.727	2.759	3.388	2.804
Na	1.245	0.646	6.910	1.290	1.280	0.706	1.196
Z	15.96	15.95	15.95	15.94	15.95	15.95	15.90
X	4.00	4.09	4.09	4.02	4.04	4.09	4.00
Ab	31.1	15.8	26	32.1	31.7	17.2	29.9
An	68.9	84.2	74	67.9	68.3	82.9	70.1

TABLE 6
Representative Olivines Analyzed by Microprobe

Sample	5-2, 134-136 cm	7-1, 106-108 cm	7-2, 42-45 cm	8-2, 43-45 cm	14-2, 113-115 cm	15-2, 79-81 cm		15-4, 114-116 cm
SiO_2	39.12	39.50	39.70	38.96	39.54	39.36	39.40	39.55
FeO^+	14.08	14.38	15.44	15.13	16.21	15.84	18.64	17.07
MgO	45.17	46.51	45.32	45.96	44.56	45.07	42.84	44.28
Total	98.37	100.39	100.45	100.05	100.30	100.27	100.88	100.90
Si	0.995	0.985	0.993	0.961	0.994	0.989	0.996	0.993
Fe	0.299	0.300	0.323	0.318	0.341	0.333	0.394	0.358
Mg	1.712	1.729	1.690	1.722	1.671	1.688	1.614	1.656
Σ	3.006	3.014	3.006	3.026	3.006	3.010	3.004	3.007
Fa	14.9	14.8	16	15.8	16.9	16.5	19.6	17.8
Fo	85.1	85.2	84	84.2	83.1	83.5	80.4	82.2

TABLE 6 – *Continued*

16-1, 28-30 cm	18-1, 55-57 cm		22-2, 61-73 cm	22-2, 110-120 cm		
				Core	Rim	
40.00	40.70	40.10	38.69	38.62	39.41	38.11
13.55	14.96	16.91	11.78	12.87	13.62	13.73
46.89	44.42	43.27	48.69	47.14	47.43	48.93
100.44	100.08	100.28	99.16	98.64	100.46	100.77
0.992	1.017	1.010	0.968	0.976	0.975	0.949
0.281	0.312	0.356	0.247	0.272	0.278	0.286
1.734	1.654	1.624	1.816	1.776	1.772	1.816
3.007	2.983	2.990	3.031	3.024	3.025	3.051
13.9	15.9	18	12	13.3	13.6	13.6
86.1	84.1	82	88	86.7	86.4	86.4

TABLE 7
Representative Partial Titanomagnetite Analyzed by Microprobe

Sample	14-2, 113-115 cm		15-2, 79-81 cm	
FeO^+	64.98	63.52	69.50	70.32
TiO_2	20.54	24.02	21.04	20.39
Total	85.53	87.54	90.10	90.71
Fe	6.375	5.952	6.475	6.572
Ti	1.812	2.024	1.763	1.714
Σ	8.87	7.976	8.238	8.286
(on the basis of 10 oxygens				